

1 **Emission-dominated gas exchange of elemental mercury vapor over natural surfaces in China**

2 Xun Wang^{1,2}, Che-Jen Lin^{1,3,4,*}, Wei Yuan^{1,2}, Jonas Sommar¹, Wei Zhu¹, Xinbin Feng^{1,*}

3

4 ¹ State Key Laboratory of Environmental Geochemistry, Institute of Geochemistry, Chinese
5 Academy of Sciences, Guiyang, China

6 ² University of Chinese Academy of Sciences, Beijing, China

7 ³ Center for Advances in Water and Air Quality, Lamar University, Beaumont, TX, USA

8 ⁴ Department of Civil and Environmental Engineering, Lamar University, Beaumont, TX, USA

9

10 *** Corresponding Authors:**

11 Xinbin Feng

Che-Jen Lin

12 Phone: +86-851-5895728

Phone: (409) 880-8761

13 Fax:+ 86-851-5891609

Fax: (409) 880-8121

14 Email: fengxinbin@vip.skleg.cn

E-mail: Jerry.Lin@lamar.edu

15

16 S1 An unpublished Hg concentration dataset
17 An unpublished Hg concentration dataset was collected in China in autumn of 2013 and 2014.
18 This dataset includes Hg concentration in litterfall collected under 5 predominant tree species in 4
19 national subtropical evergreen forests (Xishuangbanna: 21.68 N, 101.42 E; Jianfengling: 19.18 N,
20 109.73 E; Shenlongjia: 31.45 N, 109.91 E; Mt. Wuyi: 28.04 N, 117.57 E) and 4 national temperate
21 forests (Jixian: 36.16 N, 110.73E; Mt. Xiaolong: 34.35 N, 106.01 E; Mt. Xiaoxinganling: 47.17 N,
22 128.95 E; Mt. Taihang: 34.96 N, 112.4 E). The collection of litter samples, measurement of Hg
23 concentration and the quality control procedure have been described elsewhere (Zhou et al., 2013).
24 Briefly, litterfall samples were collected by 1 m × 1 m nylon nets (1 mm pore size) placed under
25 canopy. Hg concentration in litter was measured by a Lumex RA-915+ multifunctional Hg analyzer
26 equipped with a pyrolysis attachment.

27
28 S2 Monte Carlo simulation for Hg input through litterfall in China
29 Monte Carlo simulation is a modeling technique that relies on random sampling and
30 statistical data analysis (Raychaudhuri, 2008). In this study, Monte Carlo simulation was
31 applied to integrate the datasets of Hg concentration in litterfall and litterfall biomass to
32 produce the probabilistic Hg flux through litterfall. The simulation was carried out in 3
33 steps: creating statistical distribution using the observational data, perform random
34 sampling, and flux calculation. In the first step, Hg concentration in litters and litterfall
35 biomass production are regarded as random variables:

36 $Hg_i(\theta) = f_\theta(x_1, x_2, \dots, x_n | \theta)$

37 $Biomass_i(\beta) = f_\beta(x_1, x_2, \dots, x_n | \beta)$

38 where θ is a random variable vector for Hg concentrations in i group (ng g^{-1}); β is the
39 random variable vector for litterfall biomass production in i group ($\text{g m}^{-2} \text{ yr}^{-1}$). Function f
40 represents the associated probability density function. As such, F_θ and F_β represent the
41 respective cumulative probability distribution functions.

42 After determining the respective probability density functions of the data, an inverse

43 transformation method was utilized to generate a random sample from the probability
44 density distribution (Raychaudhuri, 2008). For example, the random sample for Hg
45 concentration (X) is generated by:

46 Generating: $U \sim U(0,1)$.

47 Returning: $X = F_\theta^{-1}(U)$.

48 Therefore, the random variable of Hg deposition flux caused by litterfall The
49 calculation for the Hg mass input through litterfall can be described as:

50 $X_{\theta,i} \sim F_\theta^{-1}$

51 $X_{\beta,i} \sim F_\beta^{-1}$

52 if $X_{\theta,i} > 0$ & $X_{\beta,i} > 0$ then

53
$$Flux = \begin{cases} X_{\theta,i}X_{\beta,i} & i \neq mixed\ forests \\ X_{\theta,green}r_{green}X_{\beta,mixed} + X_{\theta,deciduous}(1 - r_{green})X_{\beta,mixed} & \end{cases}$$

54 where r_{green} was the ratio for the green tree species in mixed forests and was assumed as
55 0.5. After 50,000 sampling iterations, the descriptive statistics and the 95% confidence
56 interval (CI) of L_i were calculated from the probability distribution of L_i . The Monte Carlo
57 simulation and Hg flux calculation was performed using MATLAB 2013a.

58 Table S1 Orthogonal Design (L₂₅(5⁶)) for WRF

59

Run Times	MP	CU	R	PBL
1	8	5	3	2
2	8	1	4	1
3	8	2	1	8
4	8	3	5	7
5	8	84	7	12
6	6	5	4	8
7	6	1	1	7
8	6	2	5	12
9	6	3	7	2
10	6	84	3	1
11	3	5	1	12
12	3	1	5	2
13	3	2	7	1
14	3	3	3	8
15	3	84	4	7
16	4	5	5	1
17	4	1	7	8
18	4	2	3	7
19	4	3	4	12
20	4	84	1	2
21	2	5	7	7
22	2	1	3	12
23	2	2	4	2
24	2	3	1	1
25	2	84	5	8

60

61 where MP: Microphysics Options, 8 means Thompson, 6 means WSM6, 3 means WSM3,
 62 4 means WSM5, 2 means Lin scheme.
 63 CU: Cumulus Parameterization Options; 1 means Kain-Fritsch; 2 means Betts-Miller-
 64 Janic; 3 means Grell-Freitas; 5 means Grell-3; 84 means New SAS (HWRF).
 65 R: Radiation Physics Options; 1 means Dudhia for ra_sw_physics and RRTM for
 66 ra_lw_physics ; 3 means CAM; 4 means RRTMG; 5 means New Goddard; 7 means
 67 FLG.
 68 PBL: PBL Physics Options; 1 means YSU; 2 means MYJ; 7 means ACM2; 8 means
 69 BouLac; 12 means GBM.

70

71 Table S2 peer-reviewed air-surfaces fluxes data. W means warm season (May-October), and C
 72 means cold season (November-April).
 73

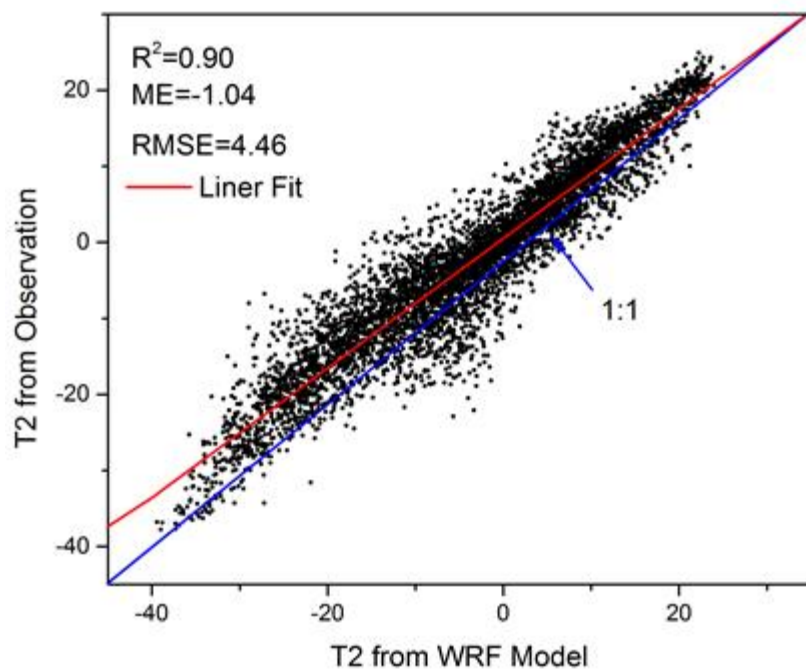
Term	Lon	Lat	Type	Flux ($\text{ng m}^{-2} \text{ h}^{-1}$)	Refencens
Paddy	106.471	26.556	W	27.4	(Wang et al., 2004)
Paddy	106.471	26.556	C	5.6	(Wang et al., 2004)
Agricultural land	102.115	29.648	C	-4.1	(Fu et al., 2008)
Agricultural land	102.115	29.648	W	19.2	(Fu et al., 2008)
Agricultural land	102.115	29.648	W	21.1	(Fu et al., 2008)
Agricultural land	102.115	29.648	C	-3.1	(Fu et al., 2008)
Agricultural land	102.088	29.680	W	2.9	(Fu et al., 2008)
Agricultural land	102.088	29.680	C	1.5	(Fu et al., 2008)
Agricultural land	102.088	29.680	W	2.1	(Fu et al., 2008)
Agricultural land	102.225	29.787	W	132	(Fu et al., 2008)
Agricultural land	102.168	29.607	W	24.5	(Fu et al., 2008)
Agricultural land	102.115	29.648	W	20.4	(Fu et al., 2008)
Agricultural land	112.47	23.014	C	32.1	(Fu et al., 2012)
Grassland	112.852	22.997	C	114	(Fu et al., 2012)
Agricultural land	113.082	22.534	C	23.8	(Fu et al., 2012)
Grassland	113.706	22.82	C	75.6	(Fu et al., 2012)
Grassland	114.457	23.116	C	24.4	(Fu et al., 2012)
Grassland	113.542	23.859	C	44.8	(Fu et al., 2012)
Agricultural land	113.569	24.703	C	18.2	(Fu et al., 2012)
Agricultural land	112.87	23.022	C	135	(Fu et al., 2012)
Agricultural land	112.422	23.13	C	14.2	(Fu et al., 2012)
Agricultural land	112.68	22.336	C	10.7	(Fu et al., 2012)
Agricultural land	112.924	21.874	C	2.7	(Fu et al., 2012)
Agricultural land	113.893	23.407	C	1.4	(Fu et al., 2012)
Agricultural land	113.639	24.712	C	22.8	(Fu et al., 2012)
wheat	116.600	36.950	W	61.2	(Sommar et al., 2013)
Agricultural land	29.921	106.370	W	31	(Zhu et al., 2011)
Agricultural land	29.921	106.370	W	15.1	(Zhu et al., 2011)
Paddy	106.370	29.921	W	20.6	(Zhu et al., 2013)
Paddy	106.437	29.757	W	4.63	(Zhu et al., 2013)
wheat	116.600	36.950	W	7.6	(Zhu et al., 2015)
wheat	116.600	36.950	C	2.2	(Zhu et al., 2015)
wheat	116.600	36.950	W	7.2	(Zhu et al., 2015)
wheat	116.600	36.950	C	5.3	(Zhu et al., 2015)
wheat	116.600	36.950	W	10.8	(Zhu et al., 2015)
wheat	116.600	36.950	C	9.3	(Zhu et al., 2015)

wheat	116.600	36.950	W	17.3	(Zhu et al., 2015)
Longtanzi reservoir	106.400	29.817	W	43.75	(Wang et al., 2006)
Jialing river	106.433	29.833	C	6.7	(Wang et al., 2006)
Hongfeng reservoir	106.471	26.556	W	6.5	(Feng et al., 2008)
Hongfeng reservoir	106.471	26.556	C	5.1	(Feng et al., 2008)
Hongfeng reservoir	106.471	26.556	C	1.8	(Feng et al., 2008)
Hongfeng reservoir	106.471	26.556	W	4.8	(Feng et al., 2008)
Hongfeng reservoir	106.471	26.556	W	4	(Feng et al., 2008)
Hongfeng reservoir	106.471	26.556	C	2.8	(Feng et al., 2008)
Hongfeng reservoir	106.471	26.556	C	2	(Feng et al., 2008)
Baihua Reservoir	106.531	26.689	C	3	(Feng et al., 2004)
Baihua Reservoir	106.531	26.689	W	6.39	(Feng et al., 2004)
Baihua Reservoir	106.531	26.689	W	7.43	(Feng et al., 2004)
Baihua Reservoir	106.531	26.689	W	6.62	(Feng et al., 2004)
Wujiang reservoir	106.785	27.312	W	20.1	(Fu et al., 2010)
Wujiang reservoir WJD-1	106.785	27.312	C	6.2	(Fu et al., 2010)
Wujiang reservoir	106.785	27.312	W	14.1	(Fu et al., 2010)
Wujiang reservoir WJD-2	106.785	27.312	C	4.7	(Fu et al., 2010)
Wujiang reservoir	106.785	27.312	W	9.9	(Fu et al., 2010)
Wujiang reservoir WJD-3	106.785	27.312	C	3.2	(Fu et al., 2010)
Wujiang reservoir	106.769	27.321	W	4.1	(Fu et al., 2010)
Wujiang reservoir SFY-1	106.769	27.321	C	1	(Fu et al., 2010)
Wujiang reservoir	106.769	27.321	W	1.5	(Fu et al., 2010)
Wujiang reservoir SFY-2	106.769	27.321	C	0.6	(Fu et al., 2010)
Wujiang reservoir	106.769	27.321	W	4.4	(Fu et al., 2010)

Wujiang reservoir SFY-3	106.769	27.321	C	1.3	(Fu et al., 2010)
Puding reservoir	105.791	26.274	W	2.2	(Fu et al., 2010)
Puding reservoir	105.791	26.274	C	0	(Fu et al., 2013b)
Puding reservoir	105.791	26.274	W	4.2	(Fu et al., 2013b)
Puding reservoir	105.791	26.274	C	0.2	(Fu et al., 2013b)
HJD-1	104.114	37.550	W	4.2	(Fu et al., 2013b)
HJD-3	104.114	37.550	W	4.2	(Fu et al., 2013b)
HJD-1	104.114	37.550	C	3.1	(Fu et al., 2013a)
HJD-2	104.114	37.550	C	2.7	(Fu et al., 2013a)
HJD-3	104.114	37.550	C	2.1	(Fu et al., 2013a)
YZD-1	105.792	26.648	W	4	(Fu et al., 2013a)
YZD-2	105.792	26.648	W	3.9	(Fu et al., 2013a)
YZD-3	105.792	26.648	W	4	(Fu et al., 2013a)
YZD-1	105.792	26.648	C	0.1	(Fu et al., 2013a)
YZD-2	105.792	26.648	C	0.4	(Fu et al., 2013a)
YZD-3	105.792	26.648	C	1	(Fu et al., 2013a)
DF Reservoir	106.180	26.859	W	3.6	(Fu et al., 2013a)
DF Reservoir	106.180	26.859	W	4.3	(Fu et al., 2013a)
DF Reservoir	106.180	26.859	W	3.3	(Fu et al., 2013a)
DF Reservoir	106.180	26.859	C	0.7	(Fu et al., 2013a)
DF Reservoir	106.180	26.859	C	0.9	(Fu et al., 2013a)
SFY Reservoir	106.769	27.321	C	3.7	(Fu et al., 2013a)
SFY Reservoir	106.769	27.321	C	2.3	(Fu et al., 2013a)
SFY Reservoir	106.769	27.321	W	4.3	(Fu et al., 2013a)
SFY Reservoir	106.769	27.321	C	1.3	(Fu et al., 2013a)
SFY Reservoir	106.769	27.321	C	1.2	(Fu et al., 2013a)
SFY Reservoir	106.769	27.321	C	1.3	(Fu et al., 2013a)
East China sea shore soil	121.898	31.054	C	3.2	Zhu et al., 2013AEa
East China sea shore soil	121.898	31.054	C	-1.4	Zhu et al., 2013AEa
Subtropical forest soil	23.178	112.544	C	6.6	(Fu et al., 2012)
Subtropical forest soil	102.020	29.703	W	6.6	(Fu et al., 2008)
Subtropical forest soil	102.143	29.420	W	5.7	(Fu et al., 2008)
Subtropical forest soil	102.111	29.628	W	9.3	(Fu et al., 2008)

Subtropical forest soil	102.063	29.603	W	7.7	(Fu et al., 2008)
Subtropical forest soil	102.030	29.588	W	0.5	(Fu et al., 2008)
Subtropical forest soil	101.930	29.583	W	2.9	(Fu et al., 2008)
Subtropical forest soil	106.656	29.609	C	0.3	(Du et al., 2014)
Subtropical forest soil	106.283	29.833	W	14.2	(Ma et al., 2013)
Subtropical forest soil	106.283	29.833	W	20.7	(Ma et al., 2013)
Simianshan forest soil	106.4333	28.583	W	7.7	(Wang et al., 2006)
Geleshan forest soil	106.417	29.567	W	3.4	(Wang et al., 2006)
Jinyunshan forest soil	106.367	29.933	W	8.4	(Wang et al., 2006)
Changbai forest	128.112	42.402	W	2.7	(Fu et al., 2015)
Forest soil	125.299	43.850	W	7.6	(Fang et al., 2003)
Forest soil	125.467	43.780	W	5.6	(Fang et al., 2003)
Forest soil	125.467	43.780	W	3.3	(Fang et al., 2003)
Grassland	102.115	29.648	C	-18.7	(Fu et al., 2008)
Grassland	102.115	29.648	C	3.1	(Fu et al., 2008)
Grassland	102.115	29.648	W	13.4	(Fu et al., 2008)
Grassland	102.115	29.648	W	12.3	(Fu et al., 2008)
Grassland	102.115	29.648	W	-1.7	(Fu et al., 2008)
Grassland	106.731	26.512	W	58.9	(Feng et al., 2005)
Grassland	106.734	26.576	W	15.4	(Feng et al., 2005)
Grassland	106.798	26.533	W	7.9	(Feng et al., 2005)
Grassland	106.798	26.533	C	2.4	(Feng et al., 2005)
Grassland	106.798	26.533	W	12.2	(Feng et al., 2005)

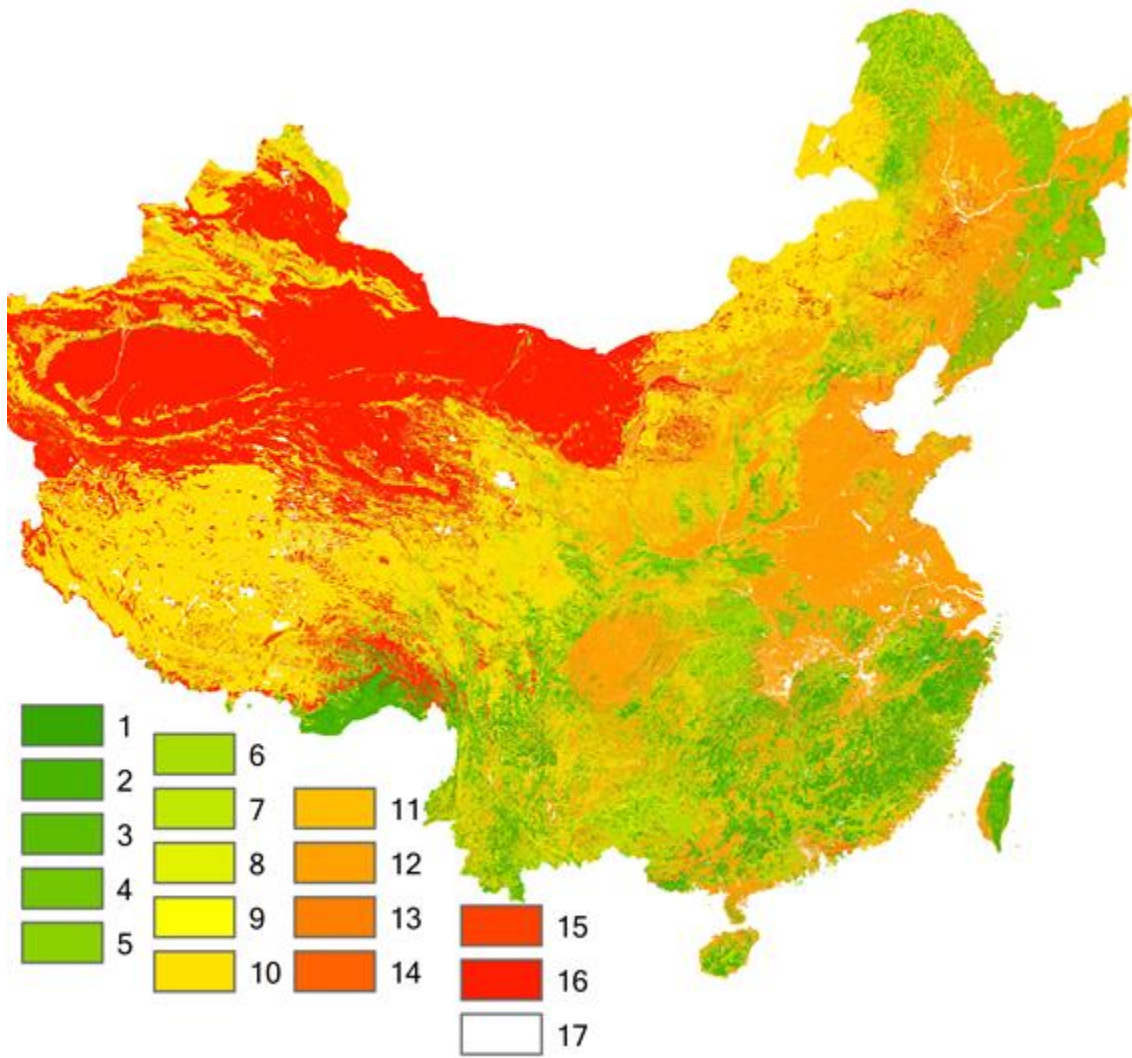
75



76

77 Figure S1 The simulated T2 (air temperature above 2 m) by WRF .vs the observed T2.

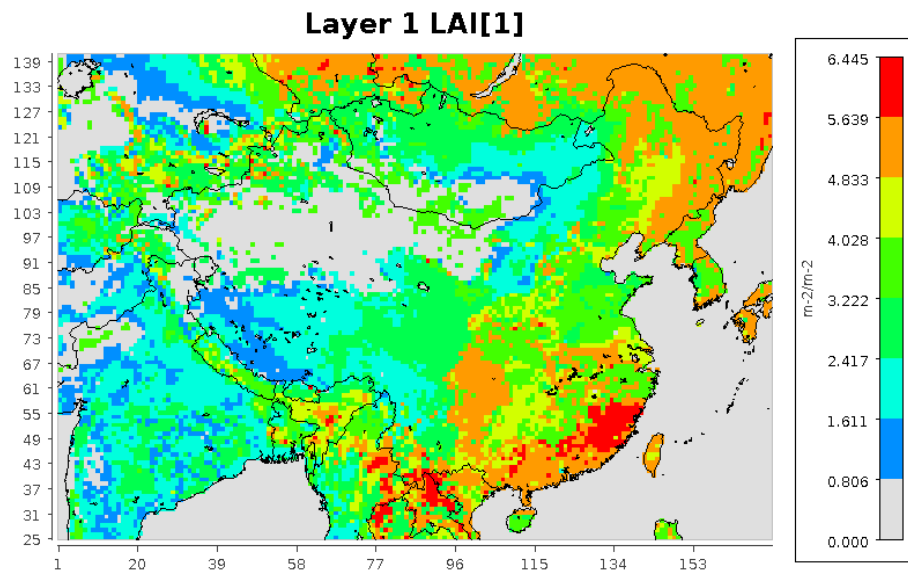
78



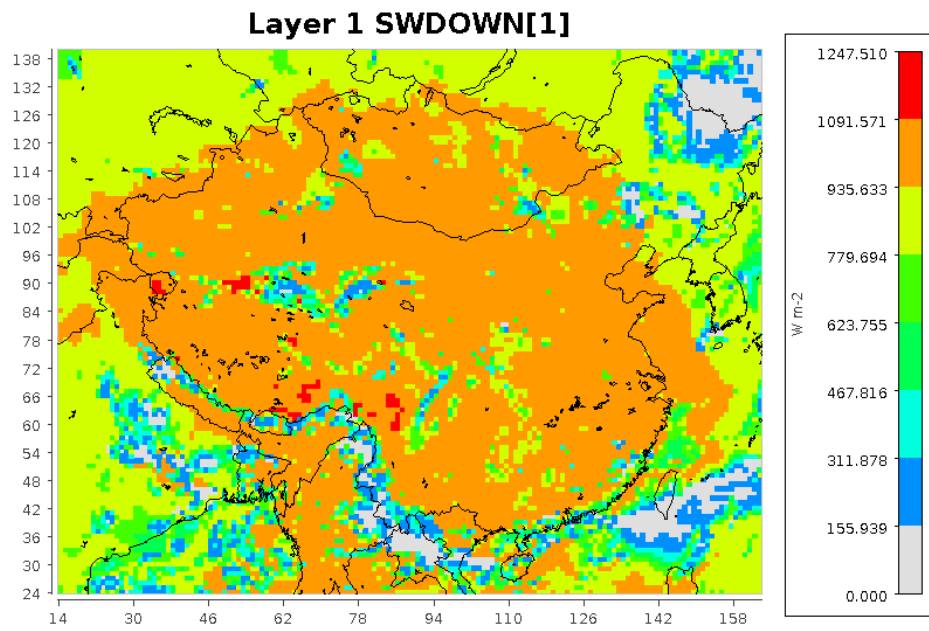
79

80 Figure S2 The spatial distribution of landuse in China. 1-17 means C1-C17.

81



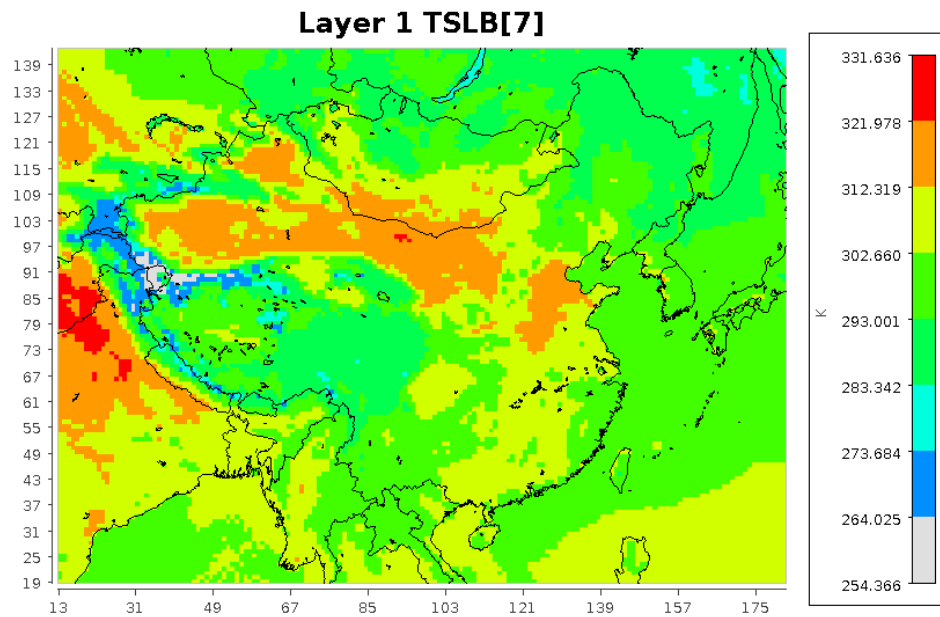
82
83 Figure S3 The spatial of mean LAI during summertime
84
85



86

87 Figure S4 The spatial distribution of mean solar radiation at 14:00 during summertime.

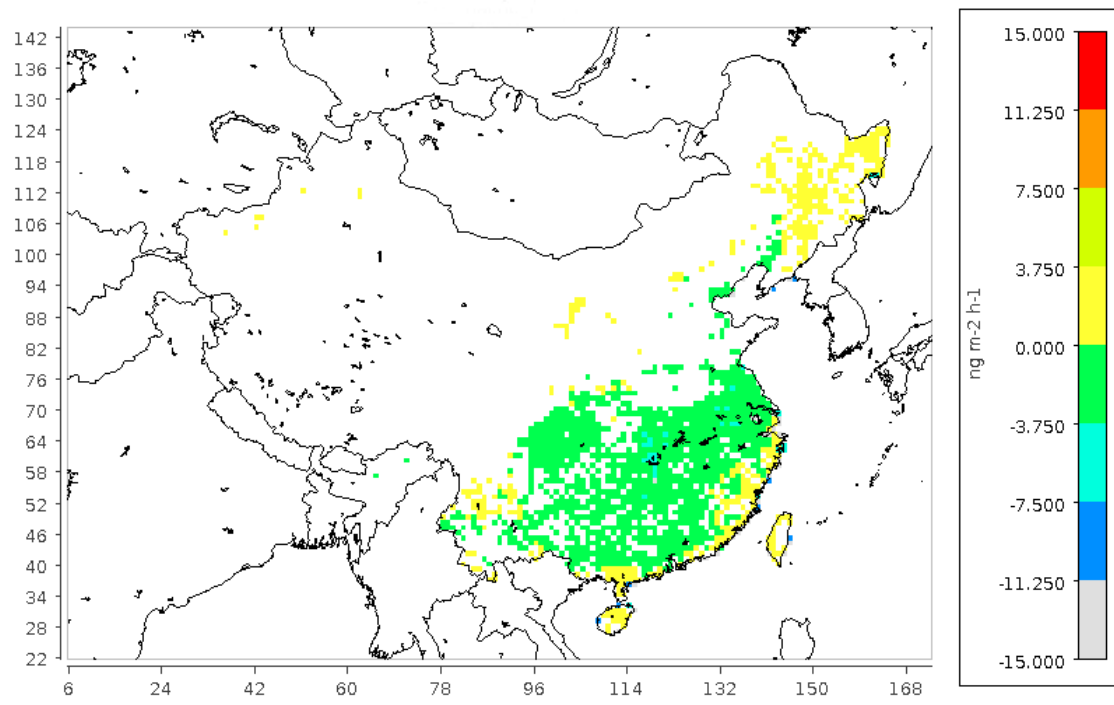
88



89

90 Figure S5 The spatial distribution of mean soil temperature at 14:00 during summertime.

91

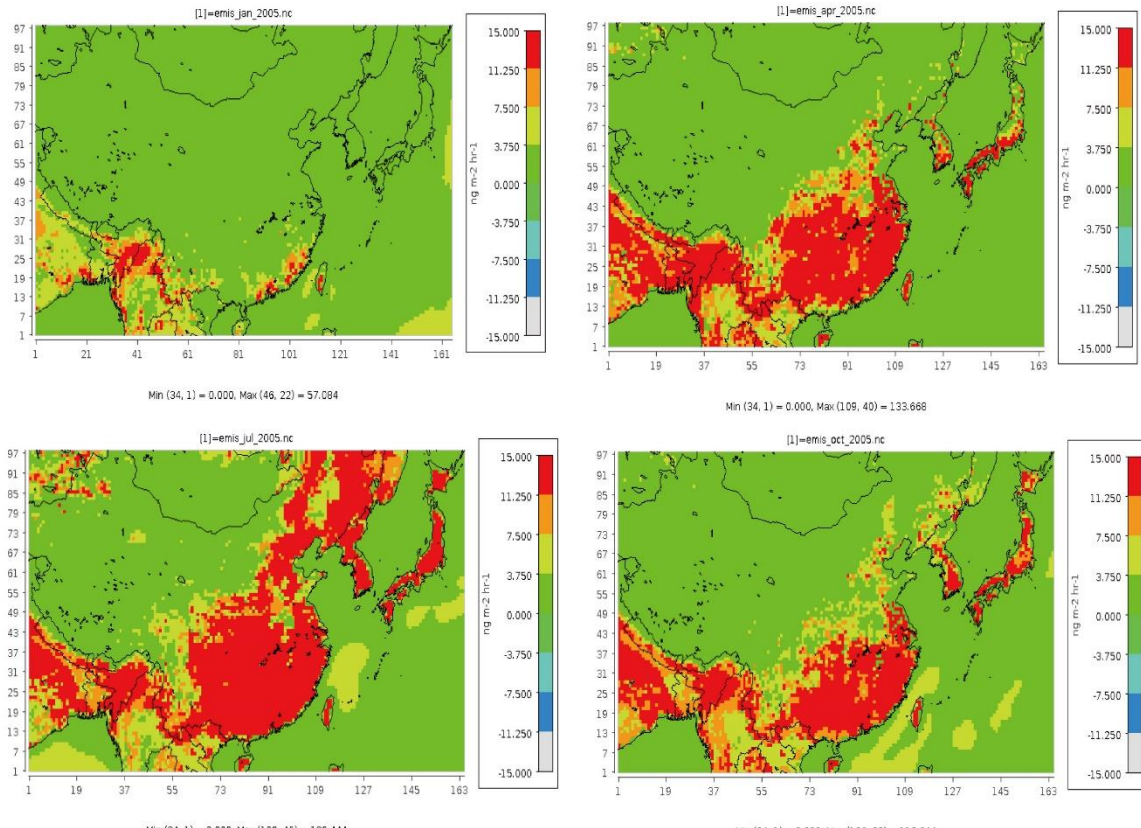


Min (115, 36) = -41.950, Max (162, 116) = 2.129

92

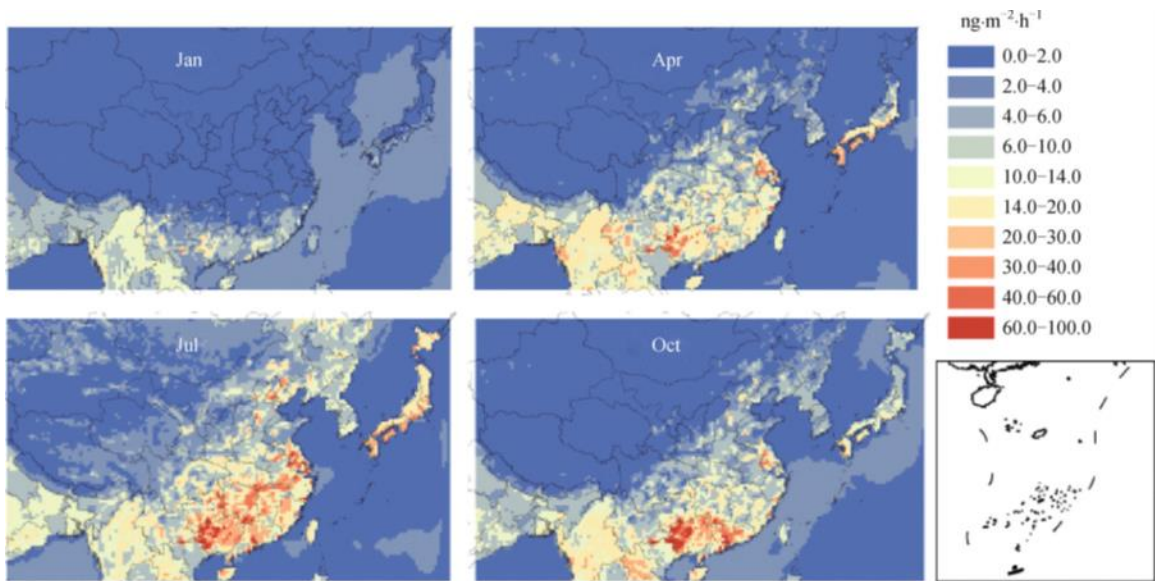
93 Figure S6. The simulated mean fluxes ($\text{ng m}^{-2} \text{ h}^{-1}$) from rice paddy during Apr-Oct.

94



95

96 Figure S7 The simulated air-surfaces Hg^0 fluxes in East Asia (Shetty et al., 2008).



97

98 Figure S8. The simulated air-surfaces Hg^0 fluxes in East Asia (Wang et al., 2014).

99

100

101

102

- 103 References
- 104 Du, B. Y., W. Q., Luo, Y., and Duan, L.: Field measurement of soil mercury emission in a Masson pine forest
105 in Tieshanping, Chongqing in Southwestern China, Huan jing ke xue= Huanjing kexue / [bian ji, Zhongguo ke
106 xue yuan huan jing ke xue wei yuan hui "Huan jing ke xue" bian ji wei yuan hui.], 35, 3830-3835, 2014.
- 107 Fang, F. M., Wang, Q. C., and Yin, J. H.: Mercury flux from urban soils and its potential factors (in Chinese),
108 Sheng Tai Huan Jing, 3, 260-262, 2003.
- 109 Feng, X. B., Yan, H. Y., Wang, S. F., Qiu, G. L., Tang, S. L., Shang, L. H., Dai, Q. J., and Hou, Y. M.: Seasonal
110 variation of gaseous mercury exchange rate between air and water surface over Baihua reservoir, Guizhou,
111 China, Atmospheric Environment, 38, 4721-4732, 2004.
- 112 Feng, X. B., Wang, S. F., Qiu, G. A., Hou, Y. M., and Tang, S. L.: Total gaseous mercury emissions from soil in
113 Guiyang, Guizhou, China, Journal of Geophysical Research-Atmospheres, 110, Artn D14306
114 Doi 10.1029/2004jd005643, 2005.
- 115 Feng, X. B., Wang, S. F., Qiu, G. G., He, T. R., Li, G. H., Li, Z. G., and Shang, L. H.: Total gaseous mercury
116 exchange between water and air during cloudy weather conditions over Hongfeng Reservoir, Guizhou, China,
117 Journal of Geophysical Research-Atmospheres, 113, 2008.
- 118 Fu, X. W., Feng, X. B., and Wang, S. F.: Exchange fluxes of Hg between surfaces and atmosphere in the eastern
119 flank of Mount Gongga, Sichuan province, southwestern China, Journal of Geophysical Research-
120 Atmospheres, 113, 2008.
- 121 Fu, X. W., Feng, X. B., Wan, Q., Meng, B., Yan, H. Y., and Guo, Y. N.: Probing Hg evasion from surface waters
122 of two Chinese hyper/meso-eutrophic reservoirs, Science of the Total Environment, 408, 5887-5896, 2010.
- 123 Fu, X. W., Feng, X. B., Zhang, H., Yu, B., and Chen, L. G.: Mercury emissions from natural surfaces highly
124 impacted by human activities in Guangzhou province, South China, Atmospheric Environment, 54, 185-193,
125 2012.
- 126 Fu, X. W., Feng, X. B., Guo, Y. N., Meng, B., Yin, R. S., and Yao, H.: Distribution and production of reactive
127 mercury and dissolved gaseous mercury in surface waters and water/air mercury flux in reservoirs on
128 Wujiang River, Southwest China, Journal of Geophysical Research-Atmospheres, 118, 3905-3917, 2013a.
- 129 Fu, X. W., Feng, X. B., Yin, R. S., and Zhang, H.: Diurnal variations of total mercury, reactive mercury, and
130 dissolved gaseous mercury concentrations and water/air mercury flux in warm and cold seasons from
131 freshwaters of southwestern China, Environmental Toxicology and Chemistry, 32, 2256-2265, 2013b.
- 132 Fu, X. W., Zhang, H., Wang, X., Yu, B., Lin, C.-J., and Feng, X. B.: Observations of atmospheric mercury in
133 China: a critical review, Atmos. Chem. Phys. Discuss., 11925-11983, doi:10.5194/acpd-15-11925-2015, 2015.
- 134 Ma, M., Wang, D. Y., Sun, R. G., Shen, Y. Y., and Huang, L. X.: Gaseous mercury emissions from subtropical
135 forested and open field soils in a national nature reserve, southwest China, Atmospheric Environment, 64,
136 116-123, 2013.
- 137 Moore, C., and Carpi, A.: Mechanisms of the emission of mercury from soil: Role of UV radiation, Journal of
138 Geophysical Research-Atmospheres, 110, 10.1029/2004jd005567, 2005.
- 139 Raychaudhuri, S.: INTRODUCTION TO MONTE CARLO SIMULATION, Proceedings of the 2008 Winter
140 Simulation Conference, 91-100, 2008.
- 141 Shetty, S. K., Lin, C. J., Streets, D. G., and Jang, C.: Model estimate of mercury emission from natural sources
142 in East Asia, Atmospheric Environment, 42, 8674-8685, DOI 10.1016/j.atmosenv.2008.08.026, 2008.
- 143 Sommar, J., Zhu, W., Shang, L. H., Feng, X. B., and Lin, C. J.: A whole-air relaxed eddy accumulation

144 measurement system for sampling vertical vapour exchange of elemental mercury, Tellus Series B-Chemical
145 and Physical Meteorology, 65, Artn 19940
146 Doi 10.3402/Tellusb.V65i0.19940, 2013.

147 Wang, D. Y., He, L., Shi, X. J., Wei, S. Q., and Feng, X. B.: Release flux of mercury from different environmental
148 surfaces in Chongqing, China, Chemosphere, 64, 1845-1854, 2006.

149 Wang, S., Zhang, L., Wang, L., Wu, Q., Wang, F., and Hao, J.: A review of atmospheric mercury emissions,
150 pollution and control in China, Frontiers of Environmental Science & Engineering, 8, 631-649,
151 10.1007/s11783-014-0673-x, 2014.

152 Wang, S. F., Feng, X. B., Qiu, G. L., and Fu, X. W.: comparision of air/soil mercury exchange
153 betwwen warm and cold season in Hongfeng reservior region, Huan jing ke xue= Huanjing kexue
154 / [bian ji, Zhongguo ke xue yuan huan jing ke xue wei yuan hui "Huan jing ke xue" bian ji wei yuan hui.], 25,
155 123-127, 2004.

156 Zhou, J., Feng, X. B., Liu, H. Y., Zhang, H., Fu, X. W., Bao, Z. D., Wang, X., and Zhang, Y. P.: Examination of total
157 mercury inputs by precipitation and litterfall in a remote upland forest of Southwestern China, Atmospheric
158 Environment, 81, 364-372, 2013.

159 Zhu, J., Wang, D., Liu, X., and Zhang, Y.: Mercury fluxes from air/surface interfaces in paddy field and dry
160 land, Applied Geochemistry, 26, 10.1016/j.apgeochem.2010.11.025, 2011.

161 Zhu, J. S., Wang, D. Y., and Ma, M.: Mercury release flux and its influencing factors at the air-water interface
162 in paddy field in Chongqing, China, Chinese Science Bulletin, 58, 266-274, 2013.

163 Zhu, W., Sommar, J., Lin, C. J., and Feng, X.: Mercury vapor air-surface exchange measured by collocated
164 micrometeorological and enclosure methods - Part I: Data comparability and method characteristics,
165 Atmospheric Chemistry and Physics, 15, 685-702, 2015.

166